the development of more efficient Hg-free fluorescent tubes and plasma display panels and has triggered the search for downconversion phosphors with quantum efficiencies that are higher than 100% in the blue and green spectral regions.

References and Notes

1. G. Blasse and B. C. Grabmaier, *Luminescent Materials* (Springer-Verlag, Berlin, 1994).
2. B. Henderson and G. F. Imbusch, *Optical Spectroscopy in Inorganic Solids* (Clarendon, Oxford, 1989).
3. C. R. Ronda, *J. Alloys Compd.* **225**, 534 (1995).
4. S. W. Depp and W. E. Howard, *Sci. Am.* **260**, 40 (March 1993).
5. F. Vollkommer and L. Hitzschke, *Phys. Bl.* **53**, 887 (1997).
6. J. L. Sommerdijk, A. Bril , A. W. de Jager, *J. Lumin.* **8**, 341 (1974); W. W. Piper, J. A. DeLuca, F. S. Ham, *ibid.*, p. 344; A. M. Srivastava, D. A. Doughty, W. W. Beers, *J. Electrochem. Soc.* **143**, 4113 (1996).
7. R. Pappalardo, *J. Lumin.* **14**, 159 (1976).
8. F. Auzel, *C. R. Acad. Sci. Paris* **262**, 1016 (1966).
9. R. T. Wegh, H. Donker, A. Meijerink, R. J. Lamminmäki, J. Hölsä, *Phys. Rev. B* **56**, 13841 (1997).
10. The energy gaps between the different ^5D_J levels of Eu^{3+} is such that four or five phonons of the highest possible energy (~500 cm^{-1} in $LiGdF_4$) are required to bridge the gap. For this situation, the radiative decay can compete with nonradiative decay to lower ^5D_J levels, and emission from all ^5D_J levels was observed.
11. J. P. M. van Vliet, D. van der Voort, G. Blasse, *J. Lumin.* **42**, 305 (1989); C. Görller-Walrand, K. Binnemans, L. Fluyt, *J. Phys. Condens. Matter* **5**, 8359 (1993).

12. The authors are grateful to P. Gürtler from Hamburger Synchrotronstrahlungslabor (HASYLAB) for the opportunity to measure at the HIGITI experimental station at the Deutsches Elektronen Synchrotron (DESY) in Hamburg, Germany. The work described here was supported by the Council for Chemical Sciences (CW), with financial aid from the Netherlands Organization for Scientific Research (NWO) and the Netherlands Foundation for Technical Research (STW). Financial support from Philips Lighting is gratefully acknowledged.

29 September 1998; accepted 15 December 1998

Argon-Lead Isotopic Correlation in Mid-Atlantic Ridge Basalts

Philippe Sarda,* Manuel Moreira,† Thomas Staudacher‡

Step-heating analyses for Mid-Atlantic Ridge glass samples show that maximum $^{40}Ar/^{36}Ar$ values correlate with $^{206,207,208}Pb/^{204}Pb$. These correlations hold for the whole Atlantic Ocean and therefore are unlikely to result from shallow-level contamination processes. Instead, they are taken as mixing hyperbolae between the degassed-depleted upper mantle and a recycled component characterized by high $^{206}Pb/^{204}Pb$ ratios (19 to 21) and low $^{40}Ar/^{36}Ar$ ratios (300 to 1000). These relations imply that argon may also be a tracer of mantle recycling.

Rare gas isotopes have been successfully used to constrain the timing of atmosphere generation by mantle degassing (*1–5*), but, except for helium (*6, 7*), they have been less useful as tracers of mantle heterogeneities, largely because of contamination by atmospheric rare gases (*8, 9*). Measuring the isotopic composition of mantle rare gases trapped in mid-ocean ridge basalt (MORB) has always met the difficulty of separating the magmatic gas from a widespread atmospheric component, a particular problem for argon. Addition of atmospheric Ar was long considered to occur during eruption on the sea floor. Indeed, the slowly cooled inner parts of submarine lava flows generally appear more contaminated than the outer layers, quenched to glass (*8, 9*). In step-heating degassing on glass samples, argon with $^{40}Ar/^{36}Ar$ ratios of 300 to 5000 is often released in the low-temperature steps (500° to 700°C). This gas is confirmation that weakly bound atmospheric argon is present in many samples (*9–13*).

In higher temperature steps, argon with high to very high $^{40}Ar/^{36}Ar$ ratios of 10,000 to 30,000 is commonly released (*9–13*). For a given sample, the maximum value obtained in a series of temperature steps is taken as the most representative of the true magmatic value, at least a minimum value because some contaminant argon may still be present. Such high $^{40}Ar/^{36}Ar$ ratios, and similar isotopic anomalies for the other rare gases, record the highly degassed character of the upper mantle (*4, 5, 9, 11*), or at least of parts of it.

Overall, $^{40}Ar/^{36}Ar$ maxima from step-heating analyses obtained for numerous mid-ocean ridge glass samples from diverse locations worldwide display a large range of values, from 500 to about 30,000 (*3, 9, 12–16*). Most authors have assumed that this variability reflects the inability of the analysis techniques to separate completely magmatic argon from contaminant argon (*9, 12, 14–16*). If this were the case, upper-mantle argon could be isotopically uniform and have a high $^{40}Ar/^{36}Ar$ signature. However, neither step-heating nor step-crushing of glass samples have ever demonstrated the existence of this single mantle argon component. In contrast, decades of improving analyses have shown that the variability of $^{40}Ar/^{36}Ar$ maxima from step-heating or crushing is the rule. Therefore, there is a possibility that this variability may be not merely due to contamination, but is at least partly inherent to mantle argon. Argon might then bear the record of some mantle heterogeneities, in the same way as Sr, Nd, or Pb.

To test this possibility, we analyzed the IPGP rare gas laboratory's large argon isotopic database for MORB to determine whether any correlation could be found between $^{40}Ar/^{36}Ar$ ratios and Pb isotope data from the literature. Initially, we used only step-heating data where more than one temperature step was performed. Samples with a $^4He/^3He$ ratio lower than 75,000 ($^3He/^4He$ higher than 9.5 Ra) were not used, as they are considered to be influenced by primitive plumes from the lower mantle. For every sample, the highest $^{40}Ar/^{36}Ar$ value from the different temperature steps was retained. When replicate argon analyses were performed, only the highest value was selected. A few samples with $^{40}Ar/^{36}Ar$ ratios lower than 1000 were discarded as possibly severely contaminated. Then, one maximum $^{40}Ar/^{36}Ar$ ratio from step-crushing was added (and one datum from total fusion). In all, 20 analyses were identified for North and South Atlantic Ocean samples having the same identification in our database for Ar and in the literature for Pb. We also included recent data for the Azores section of the Mid-Atlantic Ridge, with radiogenic lead and $^{40}Ar/^{36}Ar$ mostly lower than 1000, giving 28 samples (*17*).

The $^{40}Ar/^{36}Ar$ ratio in these samples correlates with $^{206}Pb/^{204}Pb$, $^{207}Pb/^{204}Pb$, and $^{208}Pb/^{204}Pb$ ratios. Samples with high $^{40}Ar/^{36}Ar$ ratios have typical depleted-mantle $^{206}Pb/^{204}Pb$ ratios; those with low $^{40}Ar/^{36}Ar$ have radiogenic lead (Fig. 1). The curvature of these Ar-Pb isotopic correlations is weak.

These correlations cannot reasonably be attributed, directly or indirectly, to shallow-level contamination by atmospheric argon; this would mean that the samples most contaminated in argon are the most radiogenic in Pb, for which there is no obvious reason. In the case of mixing between two magmas, it is unlikely that the magma with the most radiogenic lead would also be the most degassed (hence the most susceptible to contamination), especially over a span of 20,000 km

Laboratoire de Géochimie et Cosmochimie, Institut de Physique du Globe de Paris (IPGP), 4 place Jussieu, 75252 Paris Cedex 05, France.

*To whom correspondence should be addressed. Present address: Groupe de Géochimie des Gaz Rares, Departement de Sciences de la Terre et U.M.R. Orsayterre, Université Paris 11–Sud, 91405 Orsay Cedex, France.

†Present address: Woods Hole Oceanographic Institution, Marine Chemistry and Geochemistry, Clarke Building, 360 Woods Hole Road, Mail Stop 25, Woods Hole, MA 02543, USA.

‡Present address: Observatoire Volcanologique du Piton de la Fournaise, 14RN3, le 27e Km, 97418 La Plaine des Cafres, La Réunion, France.

along the Mid-Atlantic Ridge. Therefore, the simplest interpretation of these correlations is that they result from binary mixing between degassed-depleted mantle and another mantle component that bears radiogenic lead and low $^{40}Ar/^{36}Ar$ ratios (*18*). Osmium isotopes have also been shown to correlate with Pb isotopes (and with Sr and Nd), which permitted the discarding of interpretations of osmium isotopic variations along ridges as due to contamination by seawater osmium (*19*).

The low-$^{40}Ar/^{36}Ar$, high-$^{206}Pb/^{204}Pb$ component either could be brought up by mantle plumes or could represent the recycled part of a layered mantle. Plumes cannot be considered to originate in the lower mantle, as in our analysis we did not include samples with low $^{4}He/^{3}He$ ratios. The component with radiogenic lead and a low $^{40}Ar/^{36}Ar$ ratio must have a recycled origin (*20*). It could be carried by the present Azores or Saint Helena mantle plumes, which have a similar Pb signature considered to be recycled in origin (*21, 22*). However, the global character of the Ar-Pb isotopic correlations is more consistent with a widespread component that could be either subducted matter (*23*) or ancient plume material dispersed in the mantle (*24*).

Variability about the Ar-Pb correlations may be attributed to some remaining Ar contamination. In addition, this variability may also be related to the well-documented presence of more than two components in the mantle (*25*), although, because of the respective concentrations and isotopic compositions of Ar and Pb in the several components, Ar and Pb data reflect mixing between only two components.

We further examined other isotopic systems. Neon isotopically correlates with Pb, but we do not have enough data to draw such a conclusion. We found no correlation between helium and Pb isotopes, which is not surprising for a recycled component because air is virtually helium-free. Finally, $^{40}Ar/^{36}Ar$ and $^{87}Sr/^{86}Sr$ ratios do not correlate with each other for Atlantic samples; this is expected for a Saint Helena–type component that has a $^{87}Sr/^{86}Sr$ ratio similar to that of depleted mantle.

Some atmospheric argon should be recycled to the mantle together with subducted material, which may also be enriched in uranium (relative to Pb) and, to some extent, potassium. This recycled matter will then evolve with time as ^{206}Pb forms from decay of ^{238}U, and ^{40}Ar from decay of ^{40}K. It will thus develop radiogenic $^{206}Pb/^{204}Pb$ ratios and (depending on its $^{40}K/^{36}Ar$ ratio) a specific $^{40}Ar/^{36}Ar$ signature. Clearly, large amounts of atmospheric argon cannot have been recycled to the mantle because mantle-derived material may have high $^{40}Ar/^{36}Ar$ ratios (*26*). Recent mixing between degassed-depleted mantle and recycled components, known to occur from isotope geochemistry of Sr-Nd-Pb, should then also result in correlations between Ar and Pb isotopic ratios.

The ^{40}Ar buildup in subducted material can be described as

$$\left(\frac{^{40}Ar}{^{36}Ar}\right) = \left(\frac{^{40}Ar}{^{36}Ar}\right)_0 + \frac{\lambda_e}{\lambda_e + \lambda_\beta}\{\exp[(\lambda_e + \lambda_\beta)\Delta t] - 1\}\left(\frac{^{40}K}{^{36}Ar}\right) \quad (1)$$

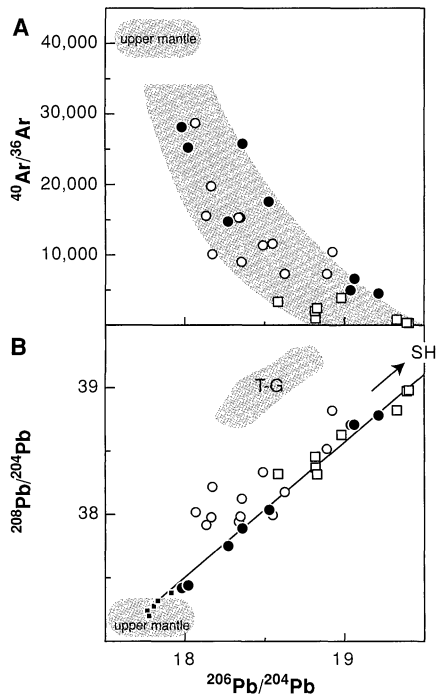

Fig. 1. (**A**) $^{206}Pb/^{204}Pb$–$^{40}Ar/^{36}Ar$ diagram for Mid-Atlantic Ridge basalt glass samples, where Ar data are from the IPGP rare gas laboratory, and Pb data are from the literature for samples with the same label (*30–35*). Argon data are maximum values from step-heating degassing of each sample (one step-crushing). Samples influenced by primitive plumes are not considered here ($^{4}He/^{3}He$ ratios are higher than 75,000). Simple binary mixing systematics are seen between degassed-depleted upper mantle and a recycled component, which indicates that recycled matter carries some amount of atmospheric argon to the mantle. Filled circles: North Atlantic Ridge; open circles: South Atlantic Ridge; open squares: Azores section of the Mid-Atlantic Ridge. (**B**) $^{206}Pb/^{204}Pb$–$^{208}Pb/^{204}Pb$ diagram displaying published data for the same Mid-Atlantic Ridge basalt samples as above, shown for reference. The main phenomenon seen is binary mixing between depleted upper-mantle Pb and a radiogenic Pb end-member attributed to a recycled mantle component, particularly manifest at Saint Helena Island (SH). T-G, Tristan and Gough islands; small filled squares, ultradepleted samples from the equatorial Mid-Atlantic Ridge (*36*); other symbols as in (A).

where λ_e and λ_β are the decay constants for electronic capture and β radioactivites of ^{40}K, respectively, and Δt is the time elapsed since subduction. To calculate the $^{40}Ar/^{36}Ar$ ratio after several thousand million years, we use $(^{40}Ar/^{36}Ar)_0 = 296$, the atmospheric value. The $^{40}K/^{36}Ar$ ratio of the recycled component is unknown, but the curvature of our Ar-Pb isotopic correlations provides some estimate of it. Using $^{40}Ar/^{36}Ar = 40{,}000$ and $^{206}Pb/^{204}Pb = 17.8$ for the depleted-degassed component, the curvature of the mixing hyperbola fitting the data in Fig. 1 depends on the $^{206}Pb/^{204}Pb$ of the recycled end-member. Assuming this recycled matter is St. Helena plume material, its $^{206}Pb/^{204}Pb$ is 21 (*27*) and the best curvature is $r = 0.15$. We then can write

$$r = \frac{(^{36}Ar/^{204}Pb)_D}{(^{36}Ar/^{204}Pb)_R} = \frac{\left(\frac{^{36}Ar}{^{40}K}\right)_D\left(\frac{^{40}K}{U}\right)_D\left(\frac{U}{^{204}Pb}\right)_D}{\left(\frac{^{36}Ar}{^{40}K}\right)_R\left(\frac{^{40}K}{U}\right)_R\left(\frac{U}{^{204}Pb}\right)_R} \approx \frac{\left(\frac{^{36}Ar}{^{40}K}\right)_D \mu_D}{\left(\frac{^{36}Ar}{^{40}K}\right)_R \mu_R} \quad (2)$$

where D and R denote depleted-degassed and recycled, respectively, and μ is the $^{238}U/^{204}Pb$ ratio.

The K/U ratio is assumed to be constant at 12,700 (*28*), or at least to differ by no more than a factor of 2 between normal ridge basalts and Saint Helena plume material (*29*). Using values of 11.0 (*29*) and 22.0 (*27*) for μ_D and μ_R, respectively, we calculate the $^{40}K/^{36}Ar$ ratio of the recycled matter to be ~3000, or one-third the value for the depleted-degassed mantle [10,000 (*4*)]. Such a low value is understandable if the recycled matter carries more atmospheric argon than potassium.

With this $^{40}K/^{36}Ar$ ratio, Eq. 1 shows that the recycled component would develop $^{40}Ar/^{36}Ar$ ratios of 530, 930, and 1640 after 1000, 2000, and 3000 million years, respectively. Such low values are consistent with the recycled end-member seen in Fig. 1.

Using a value of 19.3 (see Fig. 1) for the $^{206}Pb/^{204}Pb$ ratio of the recycled component yields a better fit with $r = 0.3$. In this case, keeping the same $^{238}U/^{204}Pb$ ratio, the $^{40}K/^{36}Ar$ ratio is 6000 and the $^{40}Ar/^{36}Ar$ ratios become 762, 1570, and 2980 after 1000, 2000, and 3000 million years, respectively. This does not change the previous conclusion.

Thus, the isotopic relations between Ar and Pb found for the Atlantic Ocean imply

that removal of the atmospheric argon contaminant by the step-heating analysis technique is sufficient to reveal that a recycled component is present at the scale of the whole ocean basin. Our data imply that atmospheric rare gases are recycled to the mantle, although in amounts weak enough not to compromise completely the isotopic signature of the degassed mantle component (*26*). Conversely, our study also supports the notion that the radiogenic lead-bearing material present in the mantle is recycled (*20*). Therefore, argon turns out to be a tracer of subduction by providing a quasi-atmospheric signature to recycled matter. Other isotopic tracers such as Pb or Sr do not retain a clear signature of their passage at the surface of Earth; for example, the buildup of ^{206}Pb in recycled sediments started well before subduction, in the crust that generated the sediments. These results could lead to a way to better quantify the amount of material recycled to the mantle and the age of recycling.

References and Notes

1. F. P. Fanale, *Chem. Geol.* **8**, 79 (1971).
2. M. Ozima, *Geochim. Cosmochim. Acta* **39**, 1127 (1975).
3. C. J. Allègre, T. Staudacher, P. Sarda, M. D. Kurz, *Nature* **303**, 762 (1983).
4. C. J. Allègre, T. Staudacher, P. Sarda, *Earth Planet. Sci. Lett.* **81**, 127 (1986–87).
5. J. Kunz, T. Staudacher, C. J. Allègre, *Science* **280**, 877 (1998).
6. M. D. Kurz, W. J. Jenkins, J.-G. Schilling, S. R. Hart, *Earth Planet. Sci. Lett.* **58**, 1 (1982).
7. D. W. Graham *et al.*, *ibid.* **110**, 133 (1992).
8. J. Dymond and L. Hogan, *ibid.* **38**, 117 (1978).
9. P. Sarda, T. Staudacher, C. J. Allègre, *ibid.* **72**, 357 (1985).
10. D. E. Fisher, *Nature* **256**, 113 (1975).
11. T. Staudacher and C. J. Allègre, *Earth Planet. Sci. Lett.* **60**, 389 (1982).
12. T. Staudacher *et al.*, *ibid.* **96**, 119 (1989).
13. M. Moreira, T. Staudacher, P. Sarda, J.-G. Schilling, C. J. Allègre, *ibid.* **133**, 367 (1995).
14. H. Hiyagon, M. Ozima, B. Marty, S. Zashu, H. Sakai, *Geochim. Cosmochim. Acta* **56**, 1301 (1992).
15. K. A. Farley and R. J. Poreda, *Earth Planet. Sci. Lett.* **114**, 325 (1993).
16. M. Moreira, J. Kunz, C. Allègre, *Science* **279**, 1178 (1998).
17. Argon and Pb data, with sample depths and locations, can be found at *Science* Online (www.sciencemag.org).
18. This model predicts that no $^{40}Ar/^{36}Ar$ ratio higher than ~3000 should ever be measured in Atlantic samples with $^{206}Pb/^{204}Pb$ ratios higher than 19.5.
19. P. Schiano, J.-L. Birck, C. J. Allègre, *Earth Planet. Sci. Lett.* **150**, 363 (1997).
20. W. M. White and A. W. Hofmann, *Nature* **296**, 821 (1982).
21. C. J. Allègre, B. Hamelin, A. Provost, B. Dupré, *Earth Planet. Sci. Lett.* **81**, 319 (1986/87).
22. A. W. Hofmann, *Nature* **385**, 219 (1997).
23. C. J. Allègre and D. Turcotte, *ibid.* **323**, 123 (1986).
24. D. Fontignie and J.-G. Schilling, *Earth Planet. Sci. Lett.* **142**, 209 (1996).
25. For example, sample AII107-7/10-1g is situated in a relatively low position in the correlation. On the basis of Pb-Nd-Sr systematics (*24, 33*), this sample reflects the influence of Gough and Tristan plumes.
26. T. Staudacher and C. J. Allègre, *Earth Planet. Sci. Lett.* **89**, 173 (1988).
27. C. Chauvel, A. W. Hofmann, P. Vidal, *ibid.* **110**, 99 (1992).
28. K. P. Jochum, A. W. Hofmann, E. Ito, H. M. Seufert, W. M. White, *Nature* **306**, 431 (1983).
29. S. Sun and W. F. McDonough, in *Magmatism in the Ocean Basins*, A. D. Saunders and M. J. Norry, Eds. (Blackwell, Oxford, 1989), vol. 42, pp. 313–345.
30. N. Machado, J. N. Ludden, C. Brooks, G. Thompson, *Nature* **295**, 226 (1982).
31. L. Dosso, H. Bougault, J.-L. Joron, *Earth Planet. Sci. Lett.* **120**, 443 (1993).
32. B. Hamelin, B. Dupré, C. J. Allègre, *ibid.* **67**, 340 (1984).
33. B. B. Hanan, R. H. Kingsley, J.-G. Schilling, *Nature* **322**, 137 (1986).
34. J. Douglass, J.-G. Schilling, D. Fontignie, *J. Geophys. Res.*, in press.
35. L. Dosso, unpublished data.
36. J.-G. Schilling, B. B. Hanan, B. McCully, R. H. Kinglsey, S. Fontignie, *J. Geophys. Res.* **99**, 12005 (1994).

37. This is contribution number 1576 of the IPGP. We thank J.-G. Schilling, who gave us the samples from the South Atlantic, and L. Dosso, who permitted us to use her unpublished Pb data for the Azores. We also thank two anonymous reviewers for their constructive comments.

5 October 1998; accepted 1 December 1998

Electrical Conductivity in the Precambrian Lithosphere of Western Canada

D. E. Boerner,* R. D. Kurtz, J. A. Craven, G. M. Ross, F. W. Jones, W. J. Davis

The subcrustal lithosphere underlying the southern Archean Churchill Province (ACP) in western Canada is at least one order of magnitude more electrically conductive than the lithosphere beneath adjacent Paleoproterozoic crust. The measured electrical properties of the lithosphere underlying most of the Paleoproterozoic crust can be explained by the conductivity of olivine. Mantle xenolith and geological mapping evidence indicate that the lithosphere beneath the southern ACP was substantially modified as a result of being trapped between two nearly synchronous Paleoproterozoic subduction zones. Tectonically induced metasomatism thus may have enhanced the subcrustal lithosphere conductivity of the southern ACP.

Petrographic, geochemical, and isotopic data indicate chemical heterogeneity in the subcontinental mantle (*1*) that is thought to result from depletion (melt extraction) and enrichment (metasomatic) events (*2*) over time. Physical samples of these mantle processes are sparsely and irregularly distributed, hampering tectonic interpretations. Upper mantle structure is more systematically revealed in global seismic tomography studies that suggest high-velocity keels (*3*) beneath Archean shields that, together with petrological data, imply an FeO poor, but olivine and orthopyroxene rich, mineralogy (*4*). How these keels have influenced, or been modified by, tectonic activity is an area of active research.

Laurentia is the Precambrian core of North America and consists of a cluster of Archean and Proterozoic provinces sutured together by extensive orogenic activity around 1900 to 1750 million years ago (Ma) (*5*) (Fig. 1). Geologic evidence of ancient convergent continental plate margins, such as fold and thrust belts and magmatic arcs, are preserved within the Proterozoic orogenic belts that surround the Archean Churchill Province (ACP) (*5*). Seismic reflection, geological, and geochemical data suggest that this Archean crust was uplifted and then reworked as a result of being trapped between two converging Paleoproterozoic orogenies (*6, 7*). As part of the LITHOPROBE Alberta Basement Transect, a magnetotelluric survey consisting of seven profiles was conducted over an area of ~550,000 km^2, covering the southern ACP and adjacent Proterozoic crust to the northwest (Fig. 1). Electromagnetic (EM) fields were recorded in the period range of 4 to 20,000 s to probe beneath the overlying veneer of conductive Phanerozoic sediments (Fig. 2, top panel). For periods of 30 to 3000 s, the EM data are dominated by the response of a number of continuous, subparallel, electrically thin yet conductive bodies between 3- and 10-km depth (top panel of Fig. 2, near sites 12 and 15). These conductors are interpreted (*8*) to represent euxinic shales, originally deposited in a Proterozoic foreland basin (*9*) and subsequently imbricated and metamorphosed at ~1850 Ma. The deeper conductors seen in the top panel of Fig. 2 are unresolvable as individual bodies and may represent mid-crustal anisotropy.

D. E. Boerner and J. A. Craven, Geological Survey of Canada, 615 Booth Street, Ottawa, Ontario K1A OE9, Canada. R. D. Kurtz and W. J. Davis, Geological Survey of Canada, 601 Booth Street, Ottawa, Ontario K1A OE8, Canada. G. M. Ross, Geological Survey of Canada, 3303 33rd Street, NW, Calgary, Alberta T2L 2A7, Canada. F. W. Jones, University of Alberta, Department of Physics, Edmonton, Alberta T6G 2J1, Canada.

*To whom correspondence should be addressed.